N.I.

WAVEFORM DISTORTION IN AN FM/FM TELEMETRY SYSTEM

by

RICHARD S. SIMPSON
RONALD C. HOUTS
and
FRED D. PARSONS

June, 1968

TECHNICAL REPORT NUMBER 14

COMMUNICATION SYSTEMS GROUP

BUREAU OF ENGINEERING RESEARCH

UNIVERSITY OF ALABAMA UNIVERSITY, ALABAMA

WAVEFORM DISTORTION IN AN FM/FM TELEMETRY SYSTEM

by

RICHARD S. SIMPSON
RONALD C. HOUTS
and
FRED D. PARSONS

June, 1968

TECHNICAL REPORT NUMBER 14

Prepared for
National Aeronautics and Space Administration
Marshall Space Flight Center
Huntsville, Alabama

Under

Contract Number NAS8-20172

Communication Systems Group
Bureau of Engineering Research
University of Alabama

ABSTRACT

A method is presented for measuring the waveform distortion in an IRIG FM/FM telemetry channel. The waveform distortion is defined as the minimum rms error between the input data signal and the signal out of the channel after compensating for any difference in amplification, dc bias, and time delay. The causes of waveform distortion in the telemetry channel and their relative importance are discussed. An experimental method for measuring the waveform distortion in the telemetry channel is developed. Results are presented for a typical channel in the form of a family of curves which display the variation of normalized waveform distortion as a function of peak-to-peak input voltage of a wideband signal using the percentage of channel bandwidth occupied by the signal as a parameter. Detailed results for 17 channels in an IRIG System are tabulated. Composite system performance is presented in the form of a curve plotting percentage waveform distortion versus percent channel utilization. This curve gives the user an approximate upper bound on signal bandwidth to insure that the waveform distortion is less than a specified percentage. Also, an average time delay for each channel is measured, and results indicate that the time delay is inversely proportional to the channel bandwidth.

ACKNOWLEDGEMENT

The authors would like to express their appreciation to the Telemetry Systems Branch, Marshall Space Flight Center, for the support of this work. In particular, Mr. Walter O. Frost and Mr. Billy M. Adair have contributed significantly to this work through the many discussions which were held at MSFC.

TABLE OF CONTENTS

LIST OF FIGURES

LIST OF SYMBOLS

A	Attenuation applied to y(t)
A_o	Optimum value of attenuation
BW	Nominal channel bandwidth
$\overline{BW}$	Data bandwidth as percent of channel bandwidth
D	Waveform distortion expressed as a % of 5 V
$E(\phi)$	RMS error signal
$E^2(\tau)$	Mean-square error between output and reference signals
$E(\tau_o, A_o)$	Minimum rms error or waveform distortion
f_d	Clock frequency
n	Total number of flip-flops in PN generator
N	Number of flip-flops in PN generator separating data and reference signal outputs
PN	Acronym for pseudo-noise
SCO	Acronym for subcarrier oscillator
τ	Time delay of the reference data signal
τ_o	Average time delay of telemetry channel
V_m	Peak-to-peak voltage of input data signal
ω_i	Angular frequency (rad/sec) where i is any subscript
x(t)	Input data signal to telemetry channel
$x(t - \tau)$	Reference signal used for comparison with y(t)
x_o	Bias applied to reference signal
y(t)	Output signal of telemetry channel

CHAPTER 1

INTRODUCTION

1.1. PURPOSE

The basic requirement for a space telemetry system is that the output signal from the ground station be an accurate representation of the input signal to the airborne package. The output signal would be an exact replica of the input signal if it were not for the waveform distortion created within the system due to such factors as nonlinearities in filter amplitude and phase characteristics, sideband clipping, crosstalk, and intermodulation distortion. Waveform distortion is defined in this report as the minimum rms value of the difference between the input and output signals after adjusting for such factors as time delay, gain, and bias. The purposes of this study were to develop a procedure for measuring rms error and using the procedure to ascertain the degree of waveform distortion for each channel of a typical IRIG FM/FM telemetry system.

The total waveform distortion was obtained by measuring the rms error for a particular channel modulated with bandlimited white noise both in the presence and absence of signals on other channels. The contributions of crosstalk and intermodulation distortion were measured by applying a dc signal to the channel under test and various test signals to the remaining channels. Finally, the distortion introduced by the channel under test was determined by applying a bandlimited white noise signal to the channel with all remaining channels turned off. The test was repeated for white noise signals employing various percentages of channel bandwidth and peak-amplitude voltage. The time delay corresponding to minimum rms error for each channel was also recorded.

The principal sources of waveform distortion in the telemetry system are discussed in the remainder of this chapter. The experimental technique for measuring distortion is presented in Chapter 2, with the results for a typical channel and overall system performance presented in Chapter 3. Appendices are included which provide details concerning a theoretical procedure for the determination of distortion for a linear system, the techniques for generating reproducible bandlimited white noise, for measuring rms error, and test results for the system.

1.2. SOURCES OF DISTORTION IN AN FM/FM SYSTEM

The analysis of the causes of waveform distortion is subdivided for discussion purposes into three parts corresponding to the relative location of the cause, i.e., distortion created in the generation, propagation, or reception of the FM/FM signal. It should be recalled that the IRIG Standards provide specifications which are designed to minimize the distortion introduced into the signal. Consequently, most of the effects discussed are presumed to be relatively small. Several attempts have been made to analyze the contributions of these various factors to waveform distortion, one of the more notable being by Crow [1] who identified some 27 sources of distortion.

1.2.1. Airborne System

The first place that waveform distortion is introduced into the data signal is in the subcarrier modulation process. The SCO lowpass filter possesses an amplitude and phase response which is not symmetrical with respect to the carrier. Consequently, sidebands above the carrier are not affected in the same manner as those below, thus creating a degree of amplitude and phase distortion. This contribution to distortion is presumed to be negligible since the carrier

fundamental and its sidebands utilize only a small portion of the filter passband near the cutoff frequency. Adair [2] has shown experimentally that the phase response across this small band is almost linear, and the error caused by phase distortion is negligible. Furthermore, his results indicate that the nonlinear amplitude response has an almost negligible effect compared to other forms of distortion. Another distortion producing feature of the SCO filter is the fact that subcarrier harmonics and their associated sidebands are not infinitely attenuated. Consequently, there is an overlap in the subcarrier spectra when the SCO outputs from the various channels are combined in the mixer. This spectral overlap is referred to as crosstalk between channels. The effect is minimized considerably since the second harmonic of the carrier is down at least 20 dB.

The mixer-amplifier and FM transmitter provide still another source of error called intermodulation distortion, which is introduced into the signal because of nonlinear transfer characteristics. A theoretical analysis of intermodulation distortion has been performed by Nichols and Rauch [3]. The nonlinear characteristics can introduce cross-modulation frequencies into the baseband spectrum which approach Gaussian noise as the number of cross-modulation terms becomes large.

1.2.2. Propagation Link

The FM signal is radiated from an antenna to a propagation medium such as the atmosphere or inter-planetary space. Distortion can be created by multipath propagation which is caused when the RF signal takes more than one path to the receiver. Another potential source of error is co-channel interference caused when two systems transmit signals of nearly identical carrier frequency in essentially the same direction. The receiving antenna cannot differentiate or select between the two signals, thus creating an error in the desired signal. These sources of waveform distortion can be reduced significantly by using

directional antennas, by making judicious assignments of carrier frequencies, and by designing receivers with good selectivity. The distortion introduced during propagation is a function of the particular transmission path and other conditions which vary from test to test. The potential contribution of distortion by the propagation medium is removed in this study by hard-wiring the transmitter and receiver through a suitable attenuator.

1.2.3. Ground Station

Since the RF receiver has good selectivity, i.e., narrow bandwidth in the tuner, there is some sideband clipping of the modulated RF carrier. Any noise created within the airborne system, transmission medium, or front end of the ground station receiver is combined with the RF signal prior to demodulation. Amplitude variation caused by the noise is eliminated in the limiter; however, phase error is not resulting in an error in the frequency. The amplitude spectrum of the demodulated noise is directly proportional to the frequency of each noise component. Assuming the interfering noise is white, the amplitude spectrum at the output of the RF receiver will be triangular in shape, increasing with frequency deviation [4]. The amplitude of the FM signals at the output of each SCO is adjusted such that each signal will have the same signal-to-noise ratio at the output of the RF receiver. This pre-emphasis decreases the adverse effects of larger noise levels for the higher channels.

Additional crosstalk is introduced by the channel-selecting bandpass filter since the attenuation is not infinite outside the passband. Some of the frequency components of the adjacent channels are transmitted in the spectrum of the desired signal. However, the bandpass filters are designed so that the amplitude response is down 20 dB at the band edge of adjacent channels. Sideband clipping is another

form of distortion caused by the bandpass filter since some of the higher-order sidebands of the FM signal are eliminated. The filter contributes further distortion due to the nonlinear amplitude and phase response in the passband.

Additional distortion is introduced by the subcarrier discriminator. The principal causes are a nonlinear frequency-amplitude transfer function and nonlinear amplitude and phase characteristics in the lowpass output filter.

CHAPTER 2

GENERAL PROCEDURE FOR MEASURING DISTORTION

For a typical FM/FM telemetry system the output will be amplified, biased, and delayed in time with respect to the input. Technically, any difference contributes to total distortion; however, these three factors are not considered to be real sources of error. The amplification factor can be eliminated by attenuating the output signal. The time delay can be eliminated from consideration by comparing the output signal with a reference signal which is a time-delayed replica of the input. The bias can be compensated by adding a dc value to the reference signal. All three factors are individually adjusted until the error is minimized. Consequently, the remaining error is attributed to waveform distortion introduced by the telemetry system.

2.1. ERROR CRITERION

There are several criteria for measuring error such as instantaneous error, mean error, rms error, etc. The most accurate error criterion is the instantaneous error since it provides an exact measure of performance for any instant in time. A probability density curve for the error could be obtained provided large numbers of instantaneous error samples were collected. From this curve the mean or variance of the error could be determined. However, obtaining this probability density curve would be very time consuming. Other criteria employ a single value to describe the system performance. Employing the mean value of the error as a criterion simplifies the analysis to the point of being meaningless, since positive instantaneous errors tend to cancel negative instantaneous errors. Consequently, a system with large instantaneous errors might appear to be quite satisfactory using this criterion. An rms error criterion appears to

be a good test for a system, since the data samples are squared before averaging is accomplished, thus insuring that positive and negative errors do not cancel. Furthermore, rms error is quite widely accepted as a suitable distortion criterion and lends itself to mathematical analysis [5]. A development of waveform distortion for a linear system based upon an rms error criterion is presented in Appendix A. This technique of analysis could be applied to a telemetry system provided a suitable mathematical model could be obtained for the system.

2.2. TEST SIGNAL

The choice of test signals is essentially unlimited, however, many bear little or no resemblance to realistic information signals. For instance, a sinusoid can be used, but since information signals are rarely sinusoidal, such a signal would have to be tediously varied in frequency across the channel bandwidth to determine the amplitude and phase characteristics of a channel intended for use with complex information signals. Triangular or rectangular test signals can also be used, but the spectral distribution of these signals is not typical of even a small class of actual information signals. In order to avoid the deficiencies of these simple signals and to produce general results, a bandlimited random signal with a uniform power density spectrum was chosen for the test signal in this work.

It is difficult using conventional diode noise sources to generate bandlimited white noise with the added requirement of accurate reproduction of the signal with a variable time delay. However, a pseudo-random noise signal, generated by passing the output from a maximum-length linear shift register [6] through a lowpass filter, can be utilized for this purpose [7]. (Details concerning the construction and characteristics of this device are presented in Appendix B.)

2 3. MEASUREMENT TECHNIQUE

The experimental technique for determining waveform distortion in a telemetry system is shown in Fig. 2.1, and follows the general approach proposed by Shepertycki [8]. Bandlimited white noise was used as a test signal for measuring the waveform distortion introduced by the channel under test. The desired bandwidth of the test signal was obtained by varying the cutoff frequency of the data filter, which is an active network consisting of an operational amplifier and an RC network. (Details concerning the design of the data filter are presented in Appendix C.) The data signal was passed through the telemetry system, while an exact replica delay delayed by τ seconds, $x(t - \tau)$, was used for comparison with the output from the system, $y(t)$. The output signal was attenuated by a factor A to compensate for the system gain, and the dc level of the reference signal was biased by an amount x_o to eliminate differences in the mean values. The mean-square value of the difference between the biased reference signal, $x(t - \tau) + x_o$, and the attenuated output signal, $A\,y(t)$, was measured using a mean-square-error device consisting of a difference amplifier and a mean-square voltmeter. (Details regarding the design of this mean-square error device are presented in Appendix D.) The values of attenuation and time delay were varied until the mean-square error was minimized. The minimum mean-square error was converted into a measure of distortion while the optimum value of time delay, τ_o, defined the average time delay [9] of the channel. (Details concerning the step-by-step procedure employed to measure distortion are presented in Appendix E.)

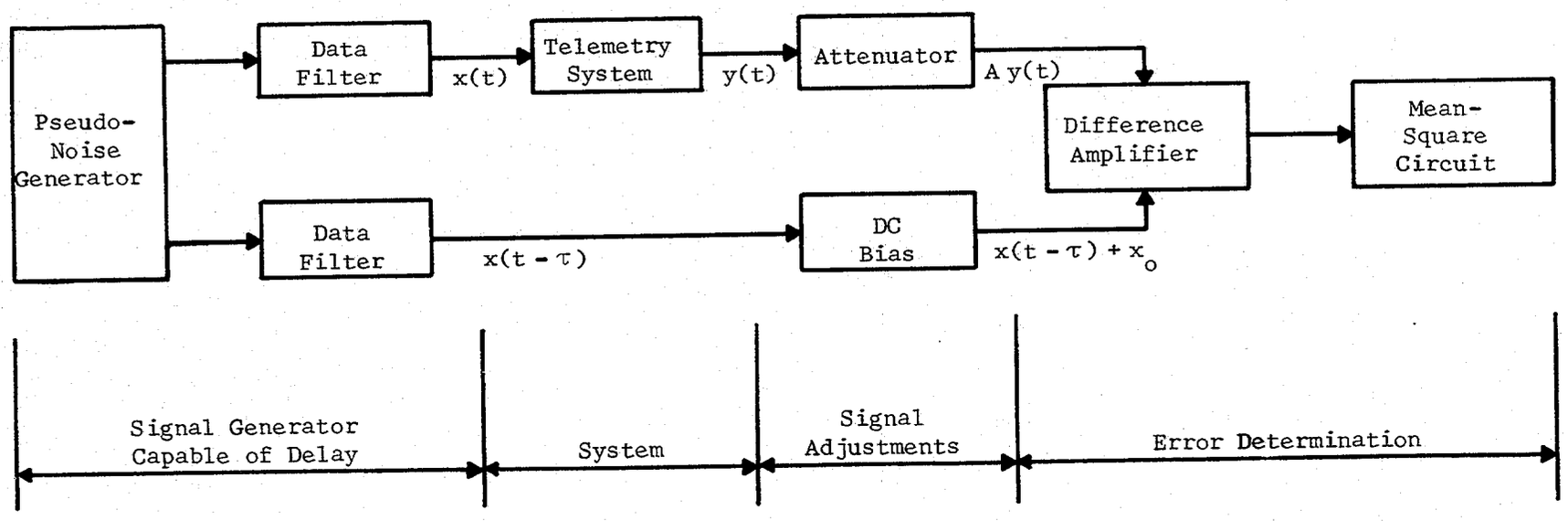

Fig. 2.1. Experimental Procedure for Measuring Waveform Distortion.

CHAPTER 3

EXPERIMENTAL RESULTS

A signal transmitted through a telemetry channel undergoes distortion caused by effects within the channel as well as inter-channel effects. Experiments were performed which isolated the contribution of inter-channel effects to total distortion. Furthermore, the bandwidth and amplitude of the test signal were both varied independently in order to identify the effect of these parameters on system performance. An average time delay for each channel was also obtained.

3.1. TEST PROCEDURE

Each of the 17 channels in an IRIG FM/FM proportional bandwidth telemetry system was tested using the scheme illustrated in Fig. 2.1. The system tested consisted of an AN/DKT-8 (XO-2) Telemetric Data Transmitting System, a Nems Clark Model 1674 FM receiver, and a Model 67F Electro-Mechanical Research subcarrier discriminator. The airborne package and ground station were connected by a cable with suitable attenuation in order to eliminate the transmission medium from consideration.

The degree of waveform distortion for a particular set of conditions was established by minimizing the error signal. The minimization was accomplished by varying the attenuation of the output and the time delay of the reference signal resulting in the optimum values of attenuation, A_o, and time delay, τ_o. The minimized mean-square error reading, $E^2(A_o, \tau_o)$, was converted to waveform distortion measured as a percentage of the maximum peak-to-peak signal (5 V) by the formula

$$D = \frac{\sqrt{E^2(\tau_o, A_o)}}{5} 100\,\%. \qquad (3.1)$$

The measurement system can indicate distortion which in reality is a result of the technique employed rather than the telemetry system. The background noise level of the measuring equipment was obtained by applying a dc signal to the channel under test and turning off the remaining channels in the telemetry system. This noise level was less than 2 mV rms, which is 0.04% of the full-scale input. By comparison, a system with 1% distortion would have an rms error of 50 mV.

Since each channel in a proportional-bandwidth IRIG FM/FM telemetry system has a different bandwidth, it is necessary that each channel be evaluated with a signal, $\overline{BW}$, bandlimited to a certain percentage of the channel bandwidth in order to correlate the data. Therefore, each channel was tested with signals having bandwidths approximating 50%, 75% and 100% of the channel bandwidth. Furthermore, the effect of peak-signal amplitude was studied by using signals, V_m, with maximum excursions ranging from 20% to 100% of the full-scale range. Each channel was tested under the aforementioned conditions both with and without modulation on the other channels in order to distinguish between the distortion contribution of the channel under test and that caused by interference from other channels.

3.2. RESULTS FOR A TYPICAL CHANNEL

The results shown in Fig. 3.1 for Channel 12 are typical. The test signal applied to the channel had a bandwidth ranging from 75 Hz to 160 Hz, the latter being the channel bandwidth, and a peak-to-peak amplitude ranging from 1 V to 5 V, increased in increments of 1 V.

3.2.1. Effects of Test Channel

The first tests performed eliminated the effects due to interference from other channels by disconnecting the SCO's for the remaining channels in the system. The essentially linear increase in distortion with signal amplitude

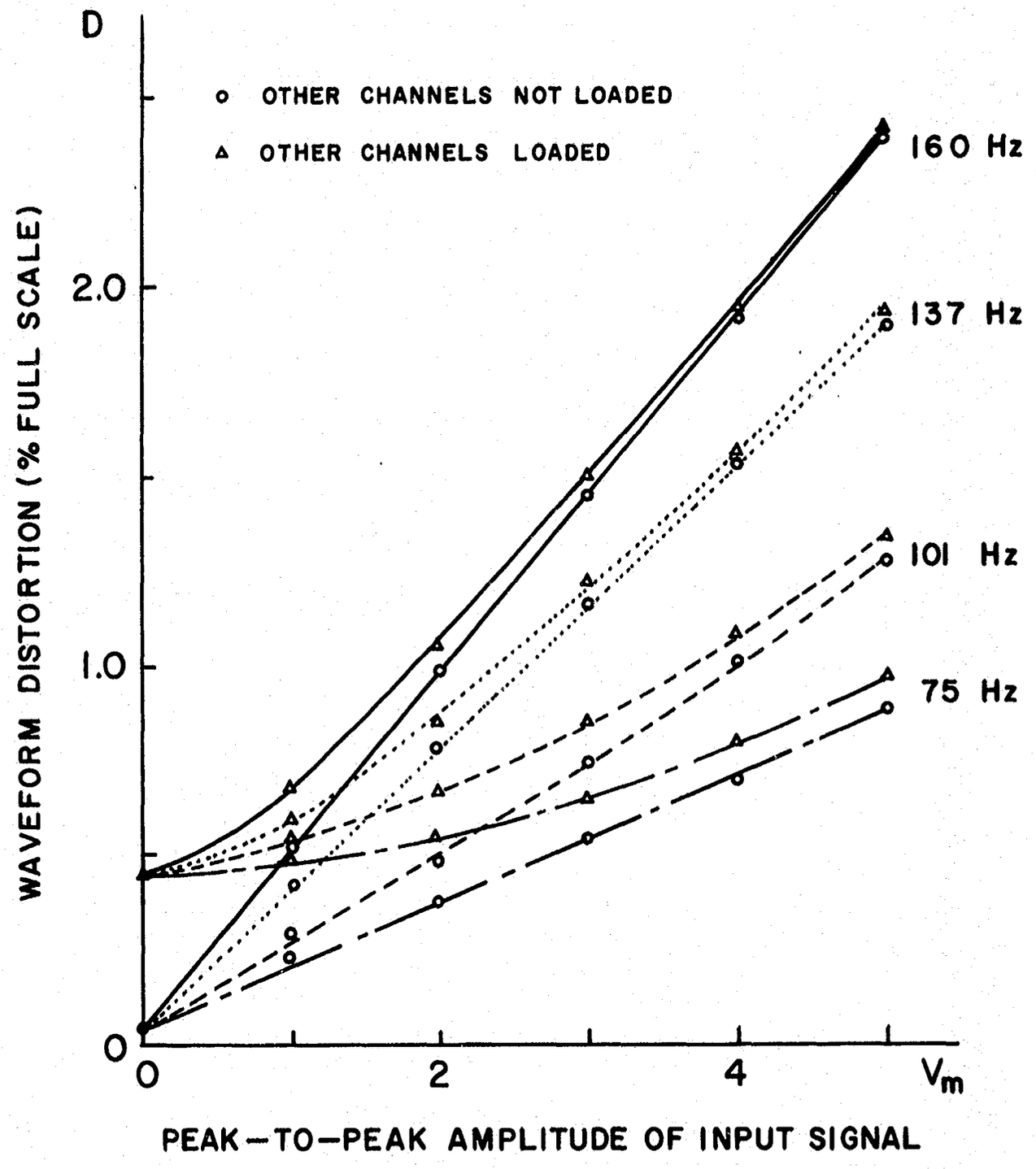

Fig. 3.1. Variation of Waveform Distortion in Channel 12. (Channel Bandwidth = 160 Hz.)

when the other channels were not modulated was a result of normalizing the distortion with respect to full-scale rather than the test-signal amplitude, which would have provided data essentially independent of signal amplitude over the operating range of the channel. The increase in waveform distortion with data bandwidth can be attributed primarily to nonlinearities in the transfer characteristics of the various filters in the system, e.g., there is considerable variation in the amplitude and phase response near cutoff of the lowpass filter in the discriminator. Furthermore, as the test signal bandwidth approached that of the channel, the 24 dB/octave skirt of the test signal spectrum was severely attenuated by the 30 dB/octave skirt of the channel beyond cutoff resulting in increased waveform distortion since the reference signal did not undergo a similar attenuation.

3.2.2. Inter-Channel Interference

It is apparent from inspection of Fig. 3.1 that the waveform distortion increased when signals were applied to the other channels. The inter-channel contribution to waveform distortion was measured by modulating all other SCO's with test signals and applying a 2.5 V dc signal to the test channel. For the experiment on Channel 12, a 5 V, 2 Hz square wave was applied to Channels 2 through 11, and a 5 V, 330 Hz sinusoid was applied to Channels 13 through 18. The distortion caused by effects from these other channels was found to have a mean-square value of 460 $(mV)^2$, or a distortion of 0.45%. Since the signals applied to these channels were not varied it would seem reasonable that this distortion contribution should be relatively independent of the test signal parameters. Indeed, the mean-square difference in distortion between readings for test channel only and readings which included the entire system for the various data bandwidths and peak-to-peak voltages had an average value of

470 $(mV)^2$, which was within 2% of the measured value without a data signal on the test channel, i.e., $V_m = 0$. The contribution of intermodulation distortion and crosstalk was obviously a larger percentage of the total distortion for data signals with low peak-to-peak amplitude and bandwidth. However, for data signals with larger peak-to-peak amplitude and bandwidth, the effect of crosstalk and intermodulation distortion appeared insignificant compared to the waveform distortion caused by test channel effects such as filter nonlinearities. This explains why the two curves corresponding to the individual channel and overall system measurements for a fixed bandwidth converged for large peak-to-peak data signals.

The information provided in Fig. 3.1 can be summarized by plotting the distortion as a function of bandwidth utilization for a 5 V peak-to-peak signal as shown in Fig. 3.2. It is apparent from this figure that the distortion increased quite markedly as the signal bandwidth approached the channel bandwidth.

3.3. SYSTEM CHARACTERISTICS

The test procedure was repeated for IRIG Channels 2 through 18. Results for signal distortion and time delay are tabulated in Appendix F for signals employing small, intermediate and large percentages of channel bandwidth.

3.3.1. Time Delay

The mean-square error scheme provides a logical measure of the average time delay for each channel, which was defined previously as that time delay required for the reference signal to minimize the rms error. The measured time delays for 15 IRIG channels corresponding to 100% bandwidth utilization are plotted as a function of channel bandwidth in Fig. 3.3. The logarithmic relation has a negative slope of unity from which it can be concluded that the time delay in each

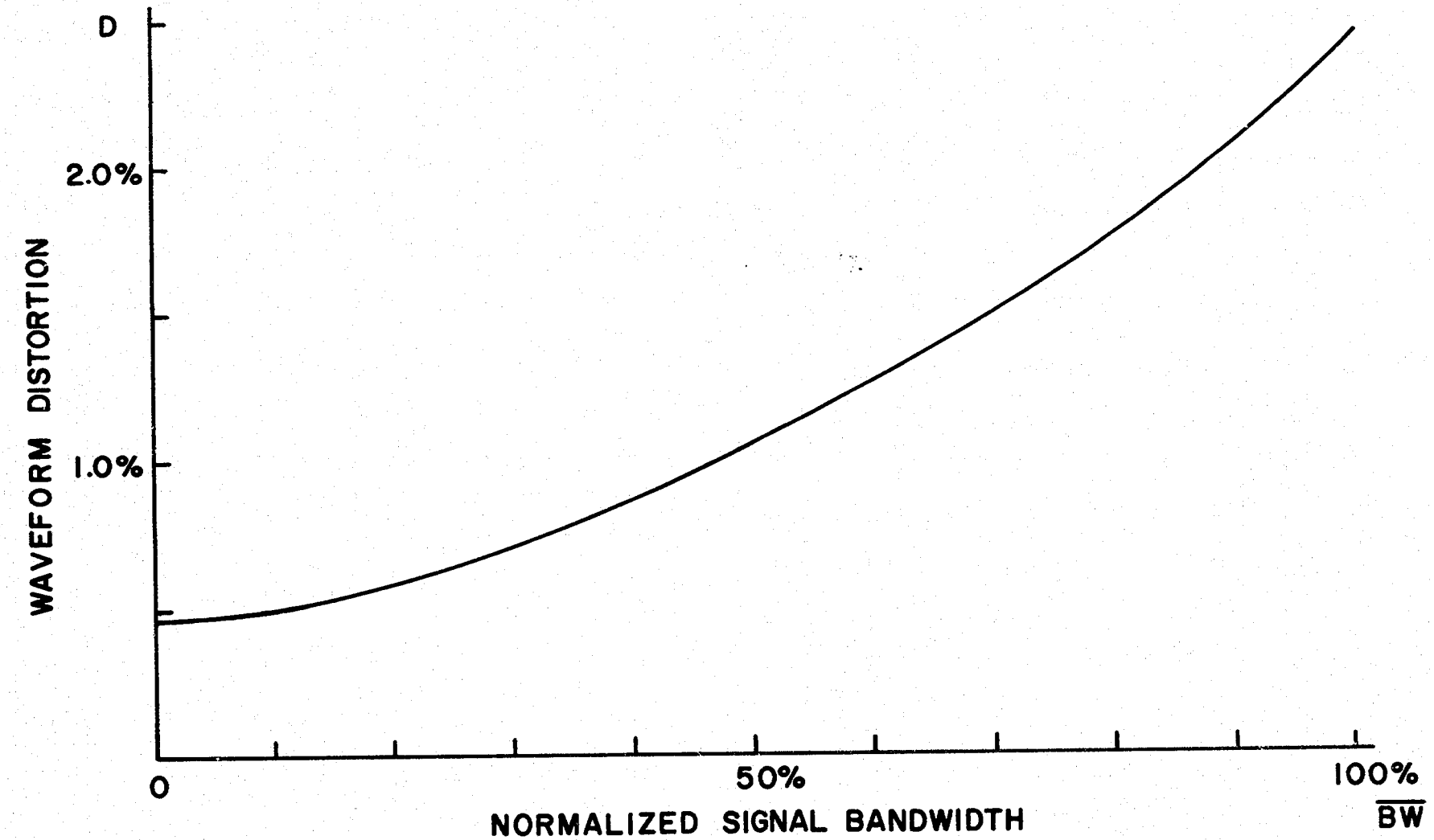

Fig. 3.2. Distortion for IRIG Channel 12.

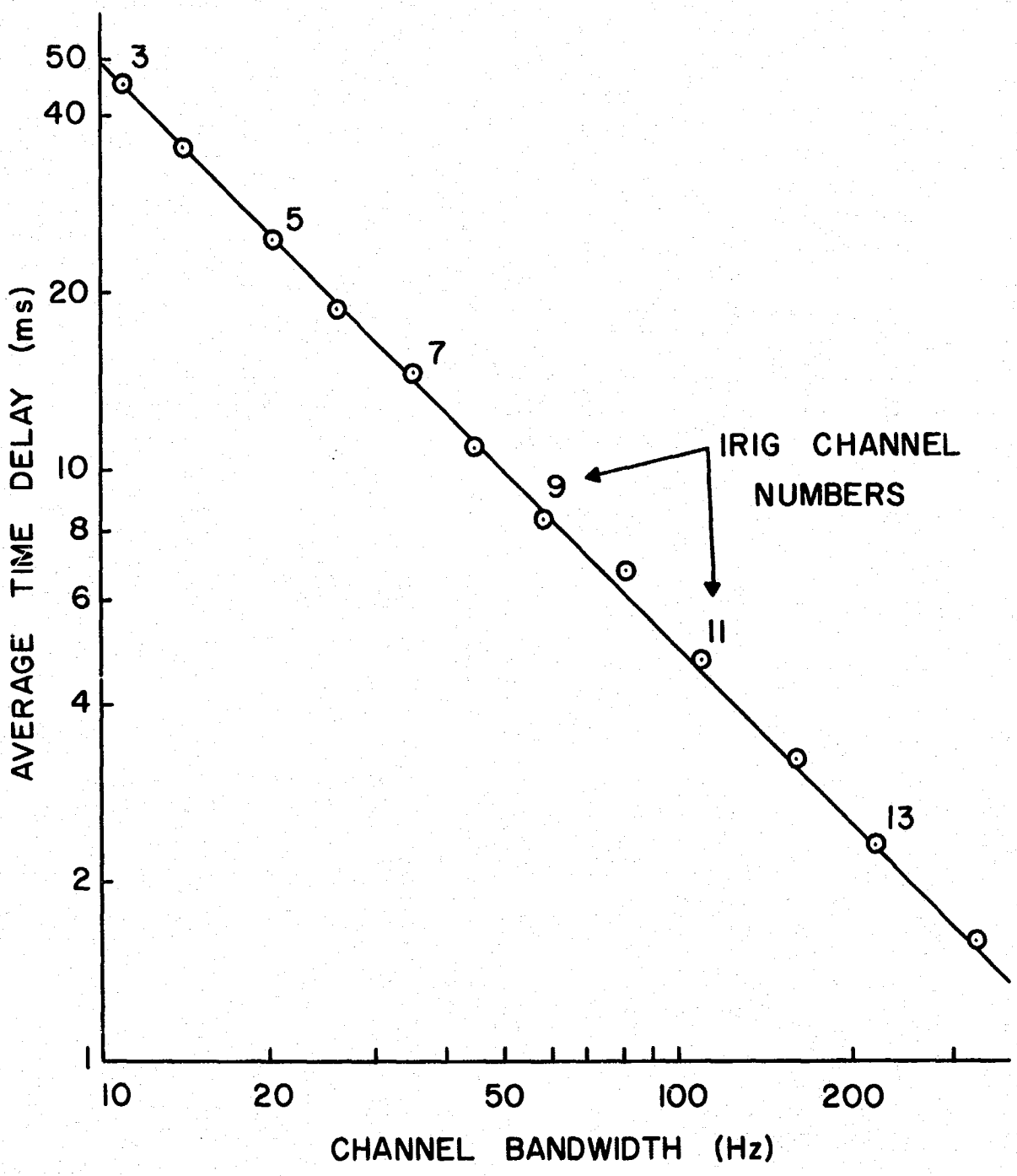

Fig. 3.3. Relationship Between Average Channel Time Delay and Channel Bandwidth for 12 IRIG Channels.

channel is inversely proportional to the channel bandwidth. The constant of proportionality is approximately 0.51 Hz · sec. Although not indicated in Fig. 3.3, inspection of the time delay data in Appendix F shows that it decreased by 5% when the bandwidth utilization was decreased to approximately 50%. The measured time delay represents an average value for minimizing error and is not the delay necessary to minimize the mean-square error caused by each frequency component in the data spectrum. The distortion is more severe for the higher frequency components which individually require larger time delays since the slope of the phase spectrum is maximum near cutoff. Consequently, the addition of higher frequency components in the test signal increased the average time delay for the system.

3.3.2. Dependence on Signal Bandwidth

The distortion data, as tabulated in Appendix F for all 17 channels and three signal bandwidths, are displayed in composite fashion in Fig. 3.4. The corridor indicated by the dotted lines defines the region within which the data points were located, and the center line of the corridor is representative, in a sense, of the overall system performance. Thus, subject to the corridor, the amount of distortion for a given signal bandwidth can be predicted to within $\pm$ 0.125% or conversely the amount of channel bandwidth utilized for a given percent of distortion can be estimated within $\pm$ 5%. Again it is apparent that the distortion increases rather sharply as the percentage of channel bandwidth utilized by the signal approaches 100%.

3.4. APPLICATION

Use of the curve in Fig. 3.4 is illustrated by the following example. Suppose it is desired to telemeter a signal with a peak-to-peak amplitude of 5 V

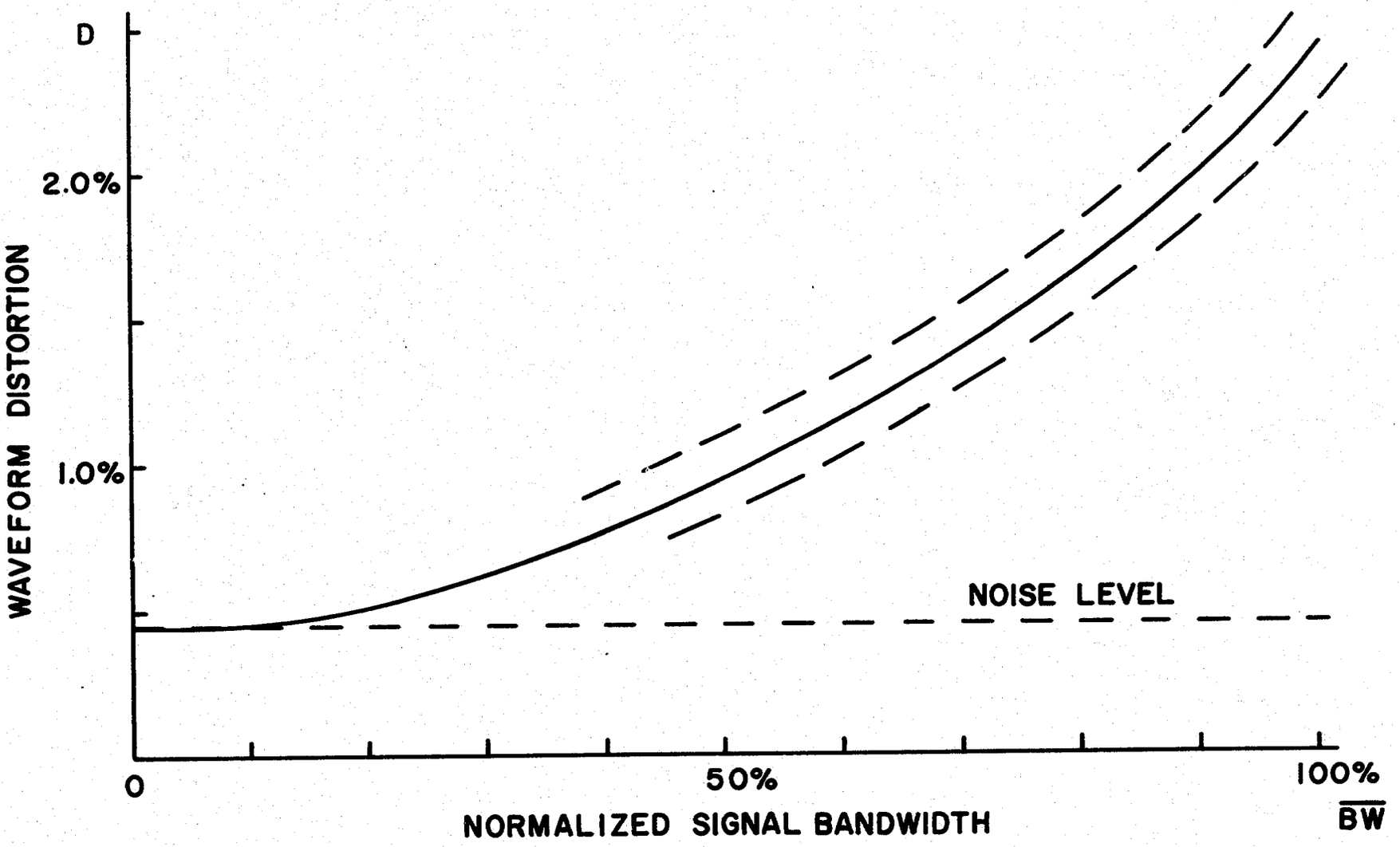

Fig. 3.4. Generalized Channel Performance for IRIG FM/FM Telemetry System.

or less and a power density spectrum flat to 100 Hz then diminishing at -24 dB/octave. It is further stipulated that the waveform distortion shall be less than 1.5%. The normalized bandwidth corresponding to this degree of distortion is found from Fig. 3.4 to be 74%. Consequently, the channel bandwidth must exceed 100/0.74 or 135 Hz. According to IRIG specifications the first channel with a bandwidth exceeding 135 Hz is Channel 12, which can be shown using the curve to result in a distortion of 1.2%. Should the requirement be restated such that the signal must be transmitted with less than 1% distortion, then the signal must be limited to 52.5% of the channel bandwidth, i.e., the channel bandwidth must exceed 190 Hz. Thus it would be necessary to transmit this signal over Channel 13, with a bandwidth of 220 Hz, resulting in a distortion of 0.85%.

CHAPTER 4

CONCLUSIONS

This report includes the results of a study on describing the performance characteristics of a telemetry channel. Both analytical and experimental techniques were investigated. It was concluded that an analytical analysis based on rms error was feasible provided a mathematical model of a telemetry channel could be obtained. Investigation of the sources of distortion in a channel led the investigators to conclude that it was not possible to derive a useful mathematical model. The experimental technique employed in this study provided the dc response needed combined with a low residual noise level on the order of 2 mV rms or 2 - 4% of the error signals being measured. The value of time delay for the reference signal required to minimize the rms error defined an average time delay for the channel.

Experimental data yielded several interesting results. The distortion in a given channel is independent of signal amplitude when normalized with respect to signal. The distortion is definitely a function of the percentage of channel bandwidth employed by the wideband test signal used, rising from 1% distortion for 50% utilization of the channel to some 2.5% for 100% utilization. The contribution due to crosstalk and intermodulation distortion was approximately 0.5% for the procedure employed, thus effectively introducing a noise threshold for the channel. The plotting of time delay versus channel bandwidth for all channels indicated that the time delay was inversely proportional to the channel bandwidth.

A graphical technique was presented for allocating wideband signals to telemetry channels. The curve employed was a display of percentage of channel bandwidth occupied versus percentage of waveform distortion. It was shown that it is possible for distortion to be reduced significantly at the expense of employing a

higher-bandwidth channel for the signal. As a rule-of-thumb for data with a 24 dB/octave skirt it appears that distortion can be kept below 1% if the channel bandwidth is twice that of the signal.

APPENDIX A

ANALYTICAL DEVELOPMENT

The rms error, $E(\tau, G)$, between the input and output of a telemetry system can be expressed as

$$E(\tau, G) = \lim_{T \to \infty} \left[\frac{1}{2T} \int_{-T}^{+T} \left[y(t) + n(t) - G\,x(t - \tau) \right]^2 dt \right]^{1/2}, \qquad (A.1)$$

where

$y(t)$ = output signal exclusive of noise,
$n(t)$ = system noise,
G = system gain,
$x(t)$ = input signal, and
τ = time delay.

Without loss of generality it is assumed that the system dc bias is zero. If the minimum value of the error is given when $\tau = \tau_o$ and $G = G_o$, waveform distortion, D, can be defined as

$$D = E(\tau_o, G_o). \qquad (A.2)$$

where τ_o is the average system time delay and G_o the average system gain. If the noise is assumed independent of $x(t)$ and $y(t)$, waveform distortion can be expressed using (A.1) as

$$D = \lim_{T \to \infty} \left[\frac{1}{2T} \int_{-T}^{+T} \left[y^2(t) + G_o^2\, x^2(t - \tau_o) - 2G_o y(t) x(t - \tau_o) + n^2(t) \right] dt \right]^{1/2}. \qquad (A.3)$$

Since the signals can be random, correlation functions [10] may be used to replace expressions involving $x(t)$ and $y(t)$ giving

$$D^2 = \phi_{yy}(0) + G_o^2\, \phi_{xx}(0) - 2G_o\, \phi_{xy}(\tau_o) + \phi_{nn}(0). \qquad (A.4)$$

If the system is modeled as being linear with a system function, $H(\omega)$, and a

corresponding unit-impulse response, h(t), (A.4) can be expressed as

$$D^2 = \frac{1}{2\pi}\int_{-\infty}^{+\infty}\left[\Phi_{xx}(\omega)\left|H(\omega)\right|^2\right]d\omega + G_o^2\,\phi_{xx}(0) - 2G_o\int_0^{+\infty}\left[h(t)\,\phi_{xx}(\tau_o - t)\right]dt + \phi_{nn}(0), \tag{A.5}$$

where $\Phi_{xx}(\omega)$ is the input power-density spectrum.

EXAMPLE

The analytical determination of waveform distortion can be demonstrated by considering the distortion introduced in an ideally-bandlimited white noise signal when passing through a noiseless system modeled as an RC lowpass filter. Such an idealized signal has a power density spectrum given by

$$\Phi_{xx}(\omega) = \begin{cases} P_d \text{ for } |\omega| < \omega_b \\ 0 \text{ for } |\omega| > \omega_b, \end{cases} \tag{A.6}$$

and a corresponding autocorrelation function

$$\phi_{xx}(t) = P\,\frac{\sin \omega_b t}{\omega_b t}, \tag{A.7}$$

where $P = \omega_b P_d/\pi$. The system function for the RC filter is

$$H(\omega) = \frac{1}{1 + j\omega RC}, \tag{A.8}$$

and the corresponding unit-impulse response is

$$h(t) = \frac{1}{RC}\,e^{-t/RC}. \tag{A.9}$$

Substituting (A.6), (A.7), (A.8), and (A.9) in (A.5), without selection of τ_o and G_o, yields

$$E^2(\tau, G) = P\left[\frac{\tan^{-1}\omega_b RC}{\omega_b RC} + G^2 - 2G\,I(\tau)\right], \tag{A.10}$$

where

$$I(\tau) = \frac{1}{RC}\int_0^{\infty}\left[e^{-t/RC}\,\frac{\sin\omega_b(\tau - t)}{\omega_b(\tau - t)}\right]dt. \tag{A.11}$$

A series solution for $I(\tau)$ can be obtained giving

$$I(\tau) = e^{-\tau/RC}\left[\frac{\tan^{-1}\omega_b RC}{\omega_b RC} + \tau/RC + \frac{2}{(2)(2!)}(\tau/RC)^2 + \frac{3 - (\omega_b RC)^2}{(3)(3!)}(\tau/RC)^3 + \frac{4 - 4(\omega_b RC)^2}{(4)(4!)}(\tau/RC)^4 + \ldots\right]. \tag{A.12}$$

It becomes apparent from inspection of (A.10) that the average system time delay, τ_o, can be found by ascertaining the value of τ which maximizes the expression for $I(\tau)$ given in (A.12). Then G_o can be found from (A.10) by substituting $I(\tau_o)$ and minimizing with respect to G using conventional calculus techniques. The rms error obtained from (A.10) and normalized with respect to signal power is plotted in Fig. A.1. The minimum of the curve defines the normalized waveform distortion and average time delay.

The problem with employing the analytical approach to analysis of a telemetry system lies in the inability to produce a proper mathematical model for the system. It would appear from experimental work that the general form would be a maximally-flat low-pass filter with a skirt of at least 30 dB/octave. However, such a model would not account for distortion caused by crosstalk, intermodulation distortion, and the other effects present in a telemetry system. No serious attempt was made to produce a mathematical model since the experimental technique appeared to produce the desired data for describing the channel characteristics. Further discussion on the analytical method and additional examples are to be found in the paper [11] by Houts and Simpson.

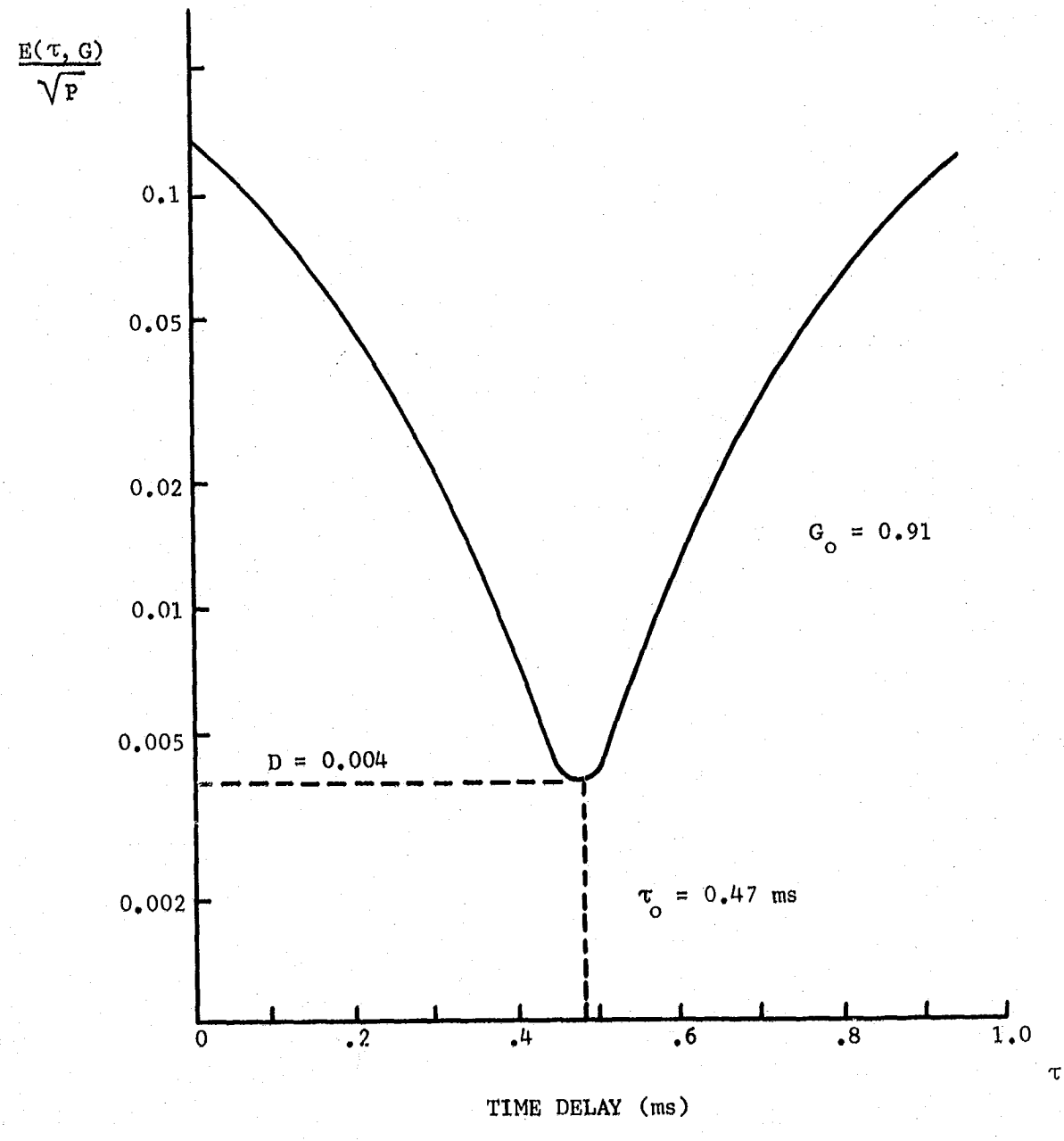

Fig. A.1. RMS Error in an RC Lowpass Filter.

APPENDIX B

TECHNIQUE FOR GENERATING PSEUDO NOISE

It is essentially impossible to generate a random noise signal which can be delayed in time without distortion. However, a pseudo-noise (PN) signal capable of being accurately delayed in time and possessing a constant power spectrum can be generated by filtering the output stage of a maximum-length linear shift register. The term pseudo-noise is used since the output of the shift register has a finite period, T, given by

$$T = \frac{2^n - 1}{f_c} \qquad (B.1)$$

where n is the number of stages and f_c is the clock frequency.

A maximum-length length linear shift register can be designed by employing a feedback pulse which is the modulo-2 sum of the outputs of the appropriate feedback stages. Tables of appropriate feedback combinations for shift registers from three to 19 stages have been derived by Davies [12]. The logic diagram for a shift register utilizing 12 stages and producing a 4095 bit sequence is given in Fig. B.1.

The clock circuit consists of a free-running multivibrator. The clock frequency can be varied by adjusting the capacitance in the feedback loop which was constructed from the parallel combination of four decades and one variable capacitor. The decades range from (0.1-0.9)μF down to (0.1-0.9)nF. Clock frequency as a function of feedback capacitance is plotted in Fig. B.2. The clock frequency and the number of flip-flop stages used to separate the data and reference signals can both be adjusted to obtain the variable time delay required for the reference signal. Changing the number of stages of delay, N, provides a coarse adjustment since one stage of delay represents a time delay equal to the recip-

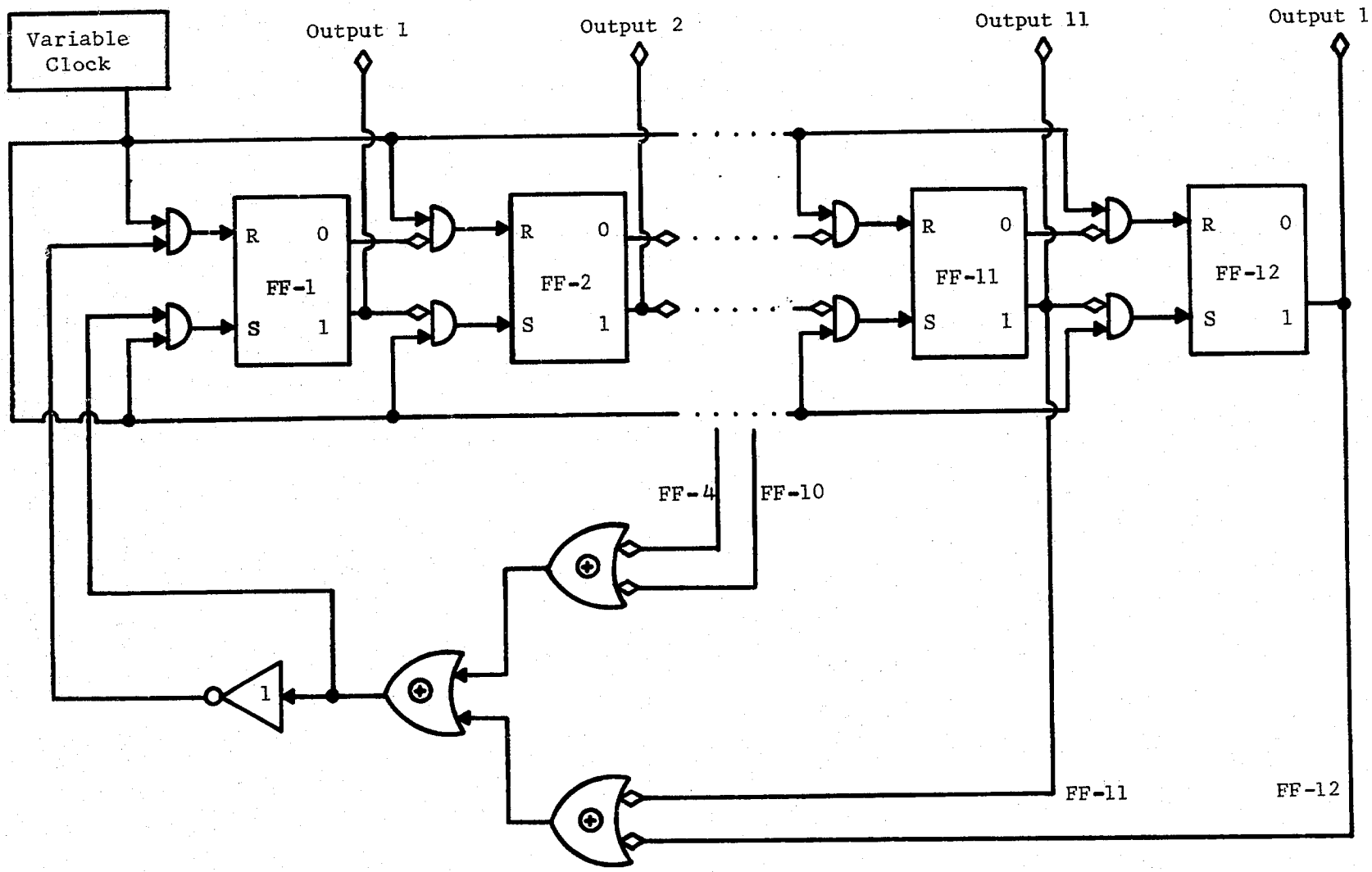

Fig. B.1. Twelve-Stage Maximum-Length Linear Shift Register.

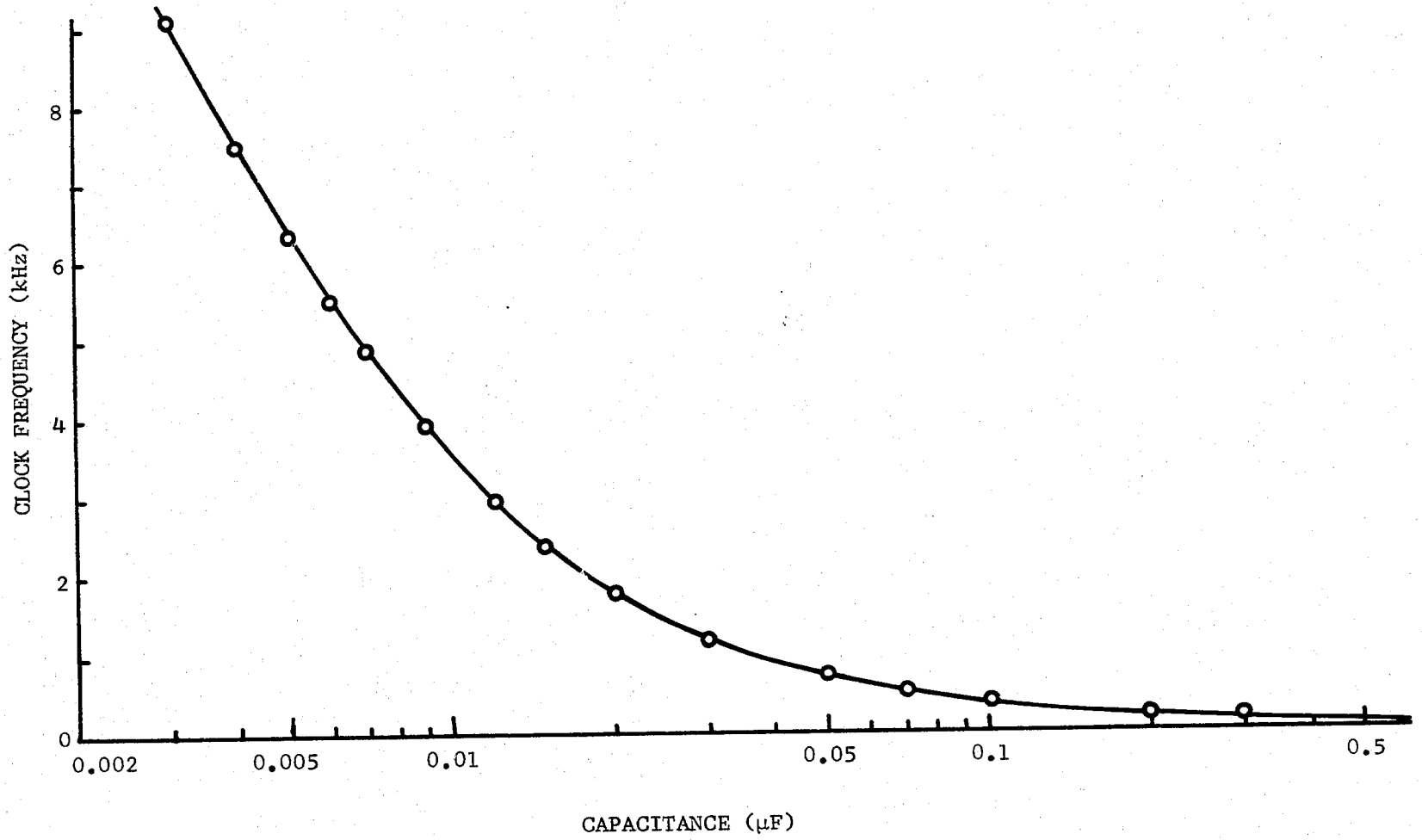

Fig. B.2. Relationship Between Clock Frequency and Feedback Capacitance.

rocal of the clock frequency. Fine adjustment in time delay is obtained by varying the clock frequency. The time delay of the reference signal, τ, can be found from the relation

$$\tau = \frac{N_d}{f_c} . \tag{B.2}$$

The square-root of the power-density spectrum of the shift register output was obtained by utilizing a General Radio spectrum analyzer. A typical result is shown in Fig. B.3 for a clock frequency of 100 Hz. The random variation in the curve is caused by the speed with which the frequency window of the analyzer sweeps across the frequency band. It can be seen that the spectrum has zeros at multiples of the clock frequency. A constant power-density spectrum for the PN signal is assured by filtering the output of the shift register with a data filter that has a cutoff frequency, f_d, which is less than one-tenth the clock frequency. A portion of the first lobe of the voltage spectrum for a 800 Hz clcok is shown in Fig. B.4. The voltage spectrum appears to be fairly constant for frequencies less than one-tenth the clock frequency. Consequently, the signal at the output of the data filter is band-limited white noise.

Gilson [13] concluded from experimental observations that the ratio f_c/f_d needs to be at least 20 to insure a gaussian amplitude density, p(X). This conclusion was investigated by following a slightly different approach. The amplitude probability density function, p(X), is related to the amplitude probability distribution, $P(\xi)$, by the derivative

$$p(X) = \frac{dP(\xi \leq X)}{d\xi} , \tag{B.3}$$

where ξ is the stationary random variable representing the amplitude. The distribution function can be obtained by measuring the percentage of time that the output signal as displayed on a strip-chart recording is less than a designated

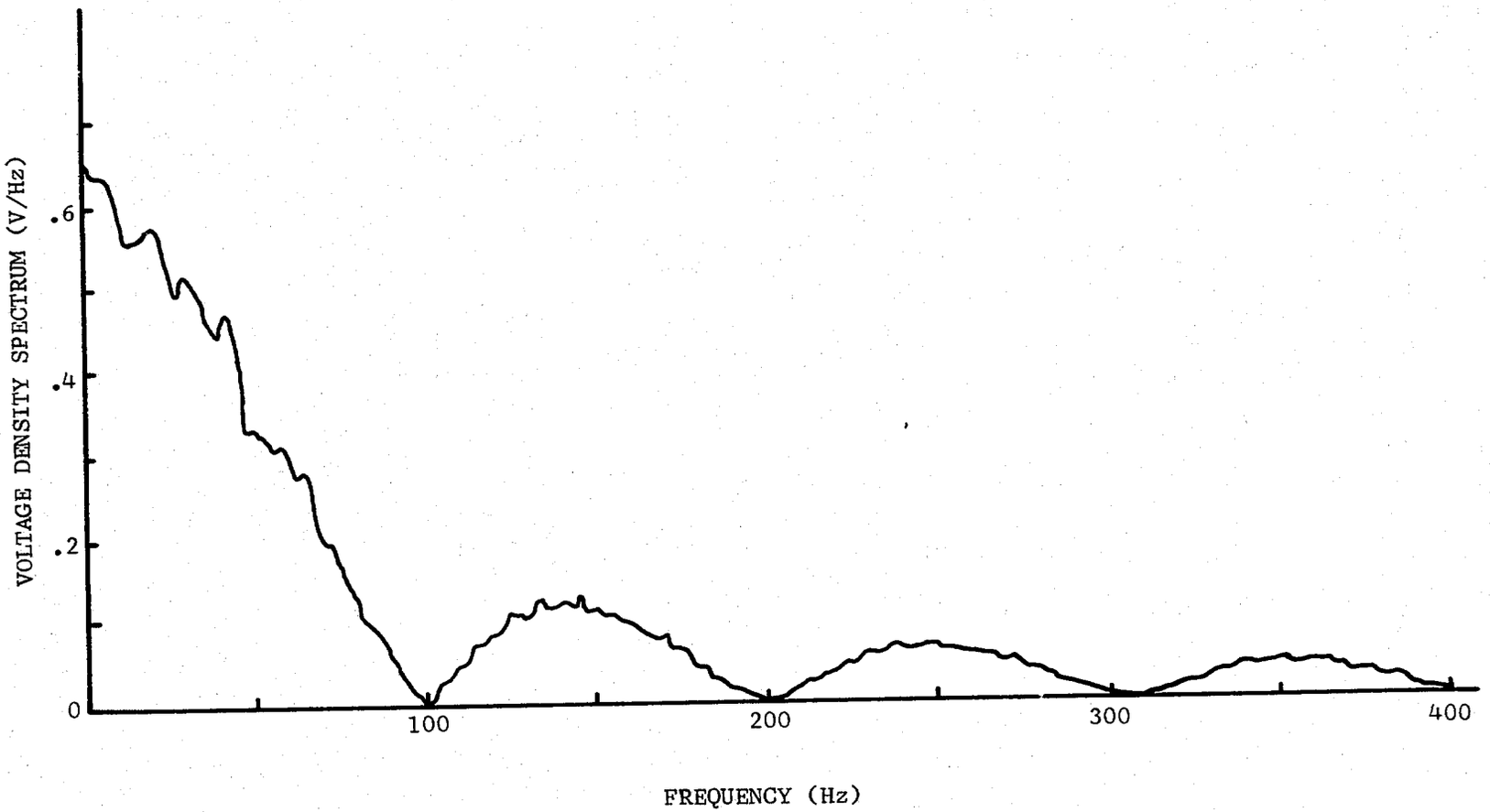

Fig. B.3. Voltage Spectrum for 100 Hz PN Sequence Generator.

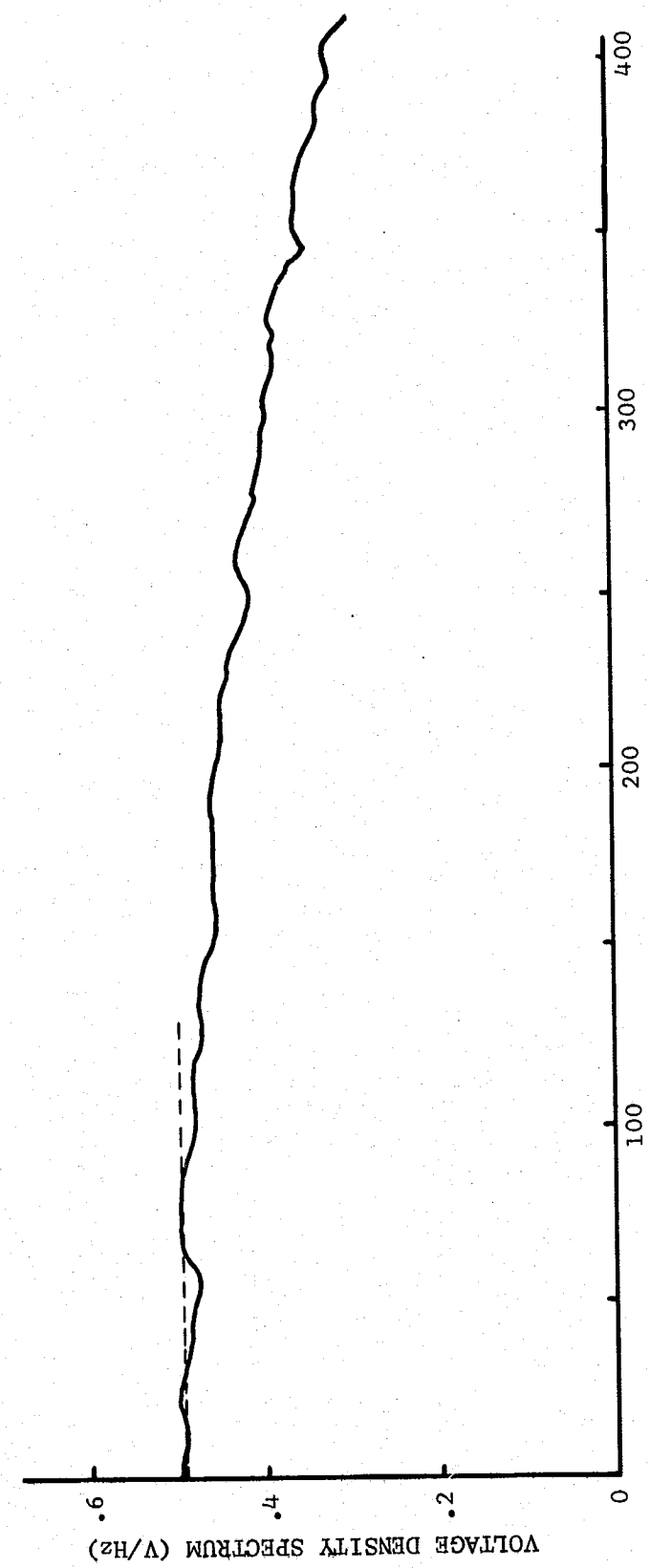

Fig. B.4. Voltage Spectrum for 800 Hz PN Sequence Generator.

value, X_o. The amplitude probability density function at X_o can be obtained graphically by measuring the slope at X_o as suggested in (B.3). The amplitude density function for f_c/f_d ratios of 5, 10, 15, and 20 were found using this method and are displayed in Fig. B.5. It can be seen from this figure that the density function already appears to be gaussian for a ratio of 15 rather than the minimum value of 20 suggested by Gilson.

A constant rms voltage level is required at the output of the data filter regardless of the clock frequency; however, the total power output for the shift register remains constant for all clock frequencies. Consequently, the percentage of power passed by the fixed data filter decreases as the clock frequency increases. This effect is demonstrated in Fig. B.6 where it is observed that the transmitted portion of the power density spectrum decreases as the clock frequency increases from f_a to f_b. Consequently, a variable attenuator is needed to maintain a constant power level based upon the amount of power available when the clock frequency is maximum for the experiment.

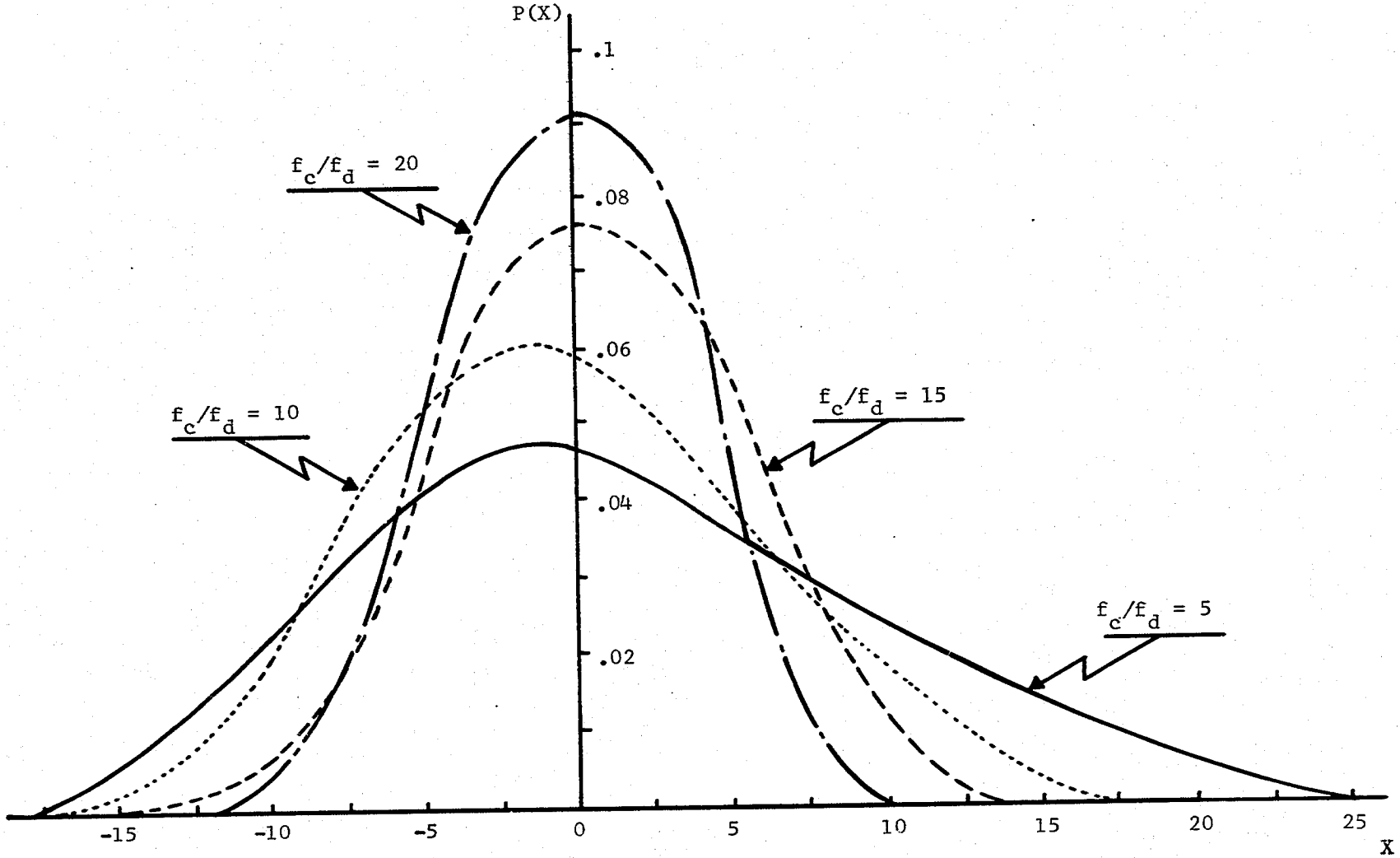

Fig. B.5. Amplitude Density Function of PN Signal for Various Clock-Filter Frequency Ratios.

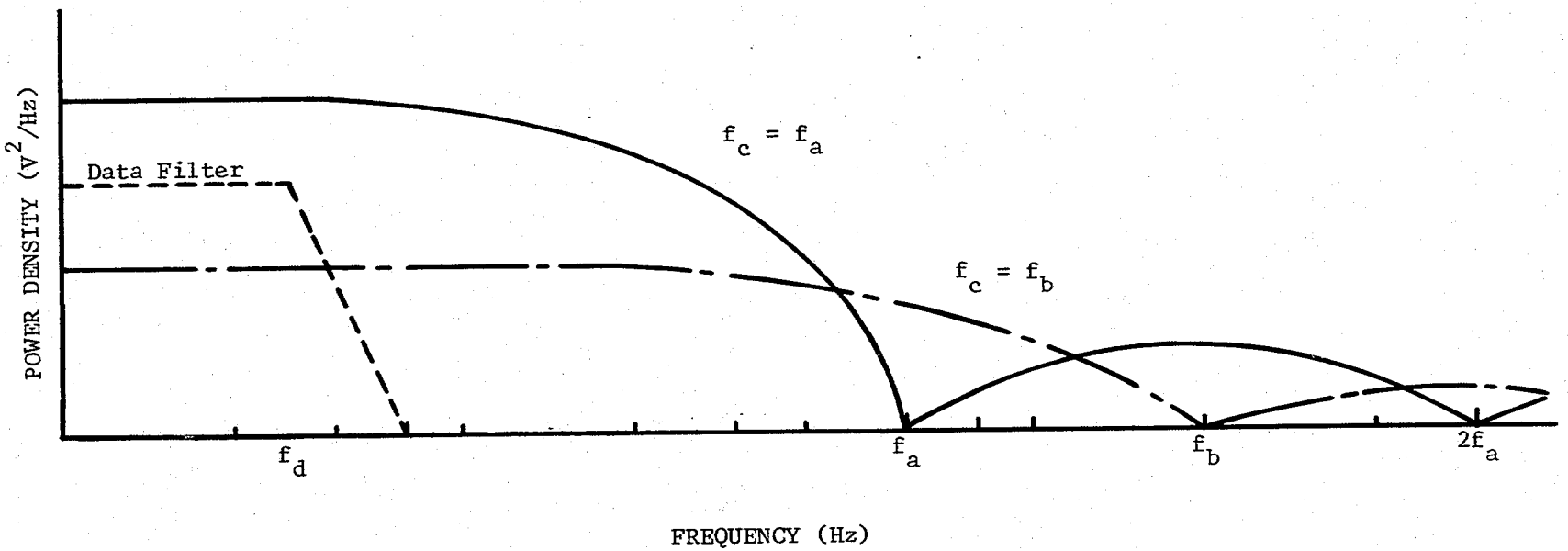

Fig. B.6. Effect of Varying Clock Frequency on Output Power Spectrum.

APPENDIX C

DATA FILTER DESIGN

The data filter used in this work was obtained by cascading two active filter sections employing operational amplifiers [14]. A circuit diagram for one filter section is shown in Fig. C.1. The transfer function, H(s), for such a filter is given by

$$H(s) = \frac{-H\,\omega_n^2}{s^2 + \alpha\omega_n s + \omega_n^2}$$

where

H = the dc gain of the amplifier,

ω_n = the filter cutoff frequency, and

α = damping constant.

The parameter values for the circuit of Fig. C.1 are determined by selecting H, ω_n, and α according to filter specifications and the capacitor, C_o, on the basis of availability. The other parameters are related to these as follows:

$$R_1 = \frac{\alpha}{2\omega_n C_o},$$

$$R_2 = \frac{R_1}{H}$$

$$R_3 = \frac{R_1}{H+1}, \text{ and}$$

$$C_4 = \frac{4(H+1)C_o}{\alpha^2}.$$

The damping constant, α, for the data filter was chosen to be $\sqrt{2}$ in order that the amplitude response be maximally flat, and the dc gain, H, was set equal to one. Each section of filter has a response which is down 3 dB at the cutoff

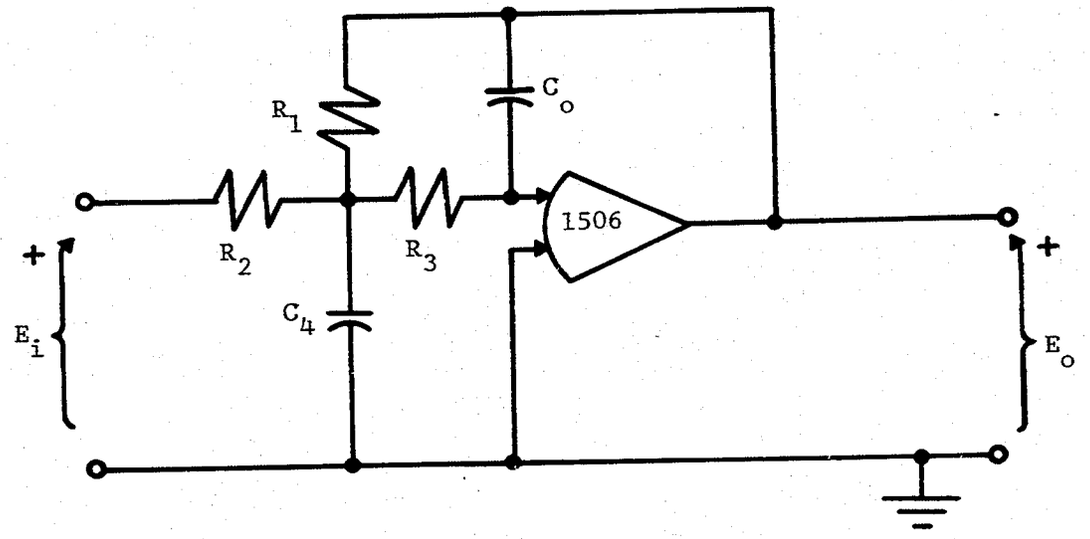

Fig. C.1. Active RC Filter Section.

frequency, ω_n, and a skirt of 12 dB/octave beyond cutoff. In a typical channel experiment the data-filter cutoff frequency was changed three or more times. One set of components is required for each change, but can be used for several experiments. (This accounts for the varying percentages of channel bandwidth utilization reported in Appendix F.) If cutoff is decreased by an order of magnitude, the same set of resistors for the new lower cutoff frequency can be used provided C_o and C_4 are increased by the same order of magnitude. The data filter had an amplitude response which was maximally flat in passband, down 6 dB at cutoff, and a skirt of 24 dB/octave beyond cutoff.

APPENDIX D

MEAN-SQUARE ERROR MEASUREMENT

Measurement of the waveform distortion requires a circuit that performs a mean-square operation upon the difference between the output of the discriminator, $y(t)$, and the delayed input, $x(t - \tau)$. The error signal can be generated by a commercial differential amplifier. However, the error signal is usually very small and approaches the noise level of the differential amplifier. A low noise difference circuit which also amplifies the error signal was designed using high-gain operational amplifiers [15]. The circuit diagram for the difference amplifier is shown in Fig. D.1. The amplified error signal, $Ke(t)$, is given by

$$Ke(t) = -\frac{R_o}{R_1}\left[x(t-\tau) - y(t)\right],$$

provided that the resistor R_1 is equal to the sum of R_2 and the in-circuit portion of R_3. The resistor R_3 is adjusted for zero output when the same signal is applied to both inputs. The ratio R_o/R_1 is selected so that the difference signal is at least 100 mV.

The mean-square value could be measured by using a differential amplifier to obtain a difference signal and then squaring the output reading from a true-reading RMS meter. Unfortunately, much of the significant error signal spectrum for lower channels is below 10 Hz, where the frequency response of commercially available RMS meters is poor. The alternative was to design a circuit to generate the mean-square error directly and measure the resultant signal using a voltmeter with dc response. A circuit which effectively measures the mean-square value of small difference signals is shown in Fig. D.2. The difference signal was still too small in some cases to properly drive the mean-square device. Consequently, the gain of Amplifier A was adjusted by proper choice of R_a in order to bring the

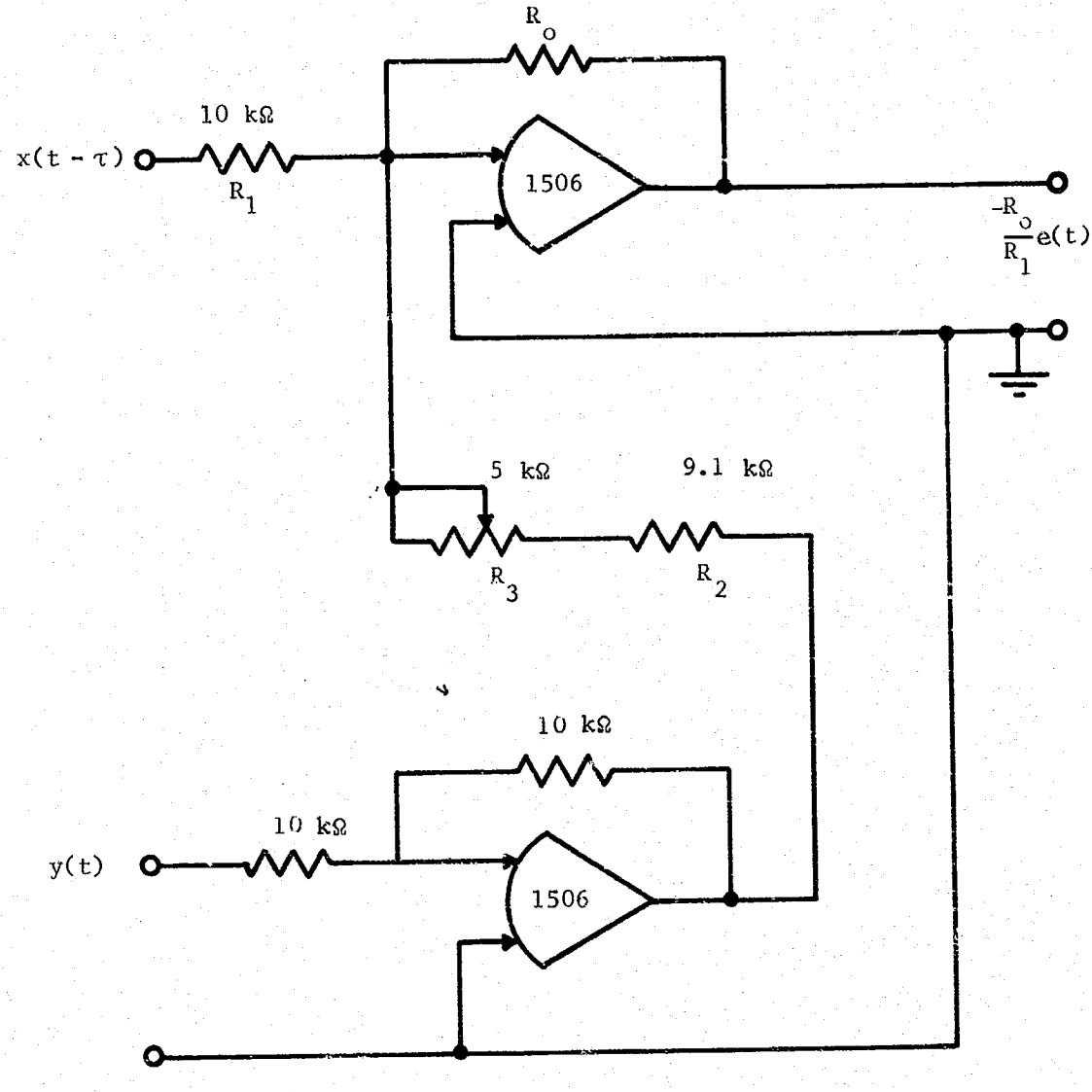

Fig. D.1. Difference Amplifier Circuit.

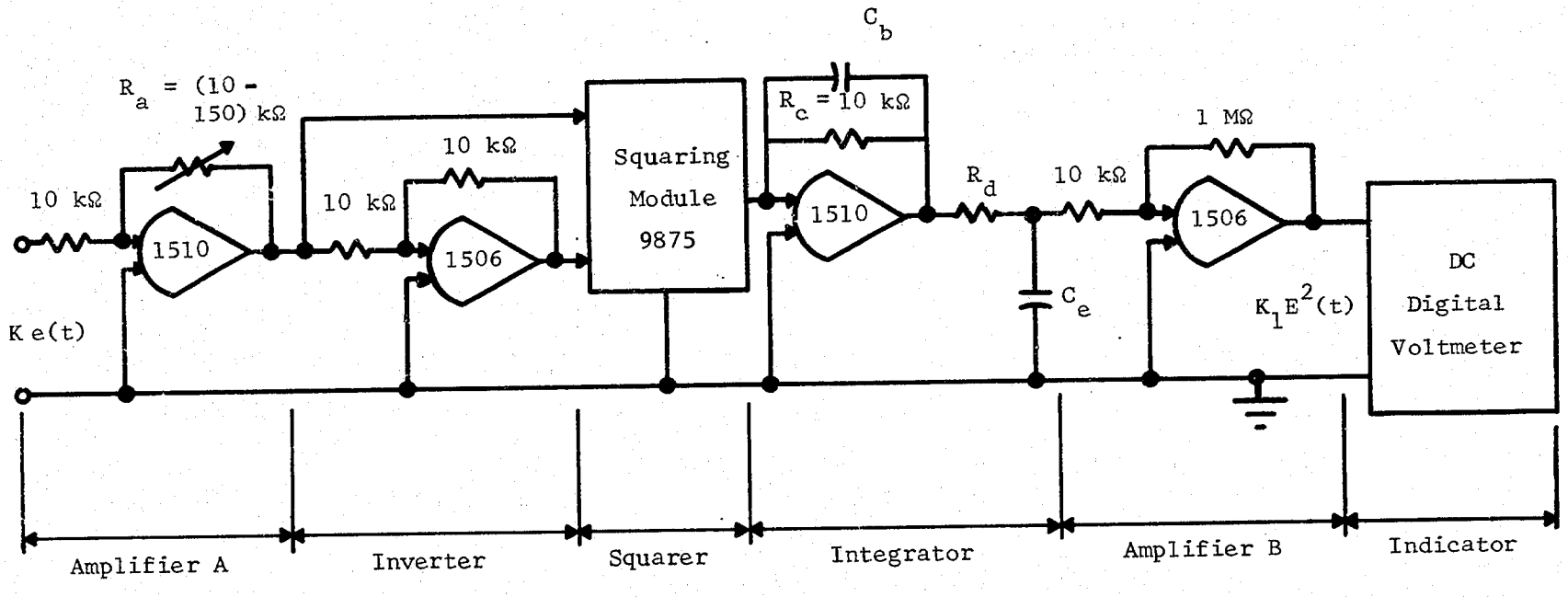

Fig. D.2. Circuit for Measuring Mean-Square Error.

difference signal to at least 1%. The negative of the error signal, which is needed for the squaring operation, was obtained by the inverter. The two signals were then applied to a squaring-module [16].

The squared signal was then averaged by the integrator whose output was proportional to the mean-square value of the error signal. The components C_b, R_c, R_d, and C_e were chosen so as to achieve a proper trade-off between measurement settling time and fluctuation in the mean-square measurement. Measurement settling time is the time needed for the mean-square value to reach its steady-state value. Theoretically, the measurement settling time would be infinite, but for practical purposes it was taken to be three time-constants, i.e., $3 R_c C_b$, resulting in a slight variation in the mean-square error readings. Thus a trade-off exists since the smaller the variation desired the longer the settling time required. The resistor R_c was fixed at 10 k Ω and C_b varied to obtain the proper trade-off. The variation in the measurement decreased with higher data bandwidths. Consequently, the settling time was shortened by making C_b smaller. Conversely, the variation increased at the lower data bandwidths, and the settling time had to be increased by making C_b larger. The lowpass filter consisting of R_d and C_e was inserted to remove any high frequency noise. The break frequency of this filter was chosen to be 1 Hz.

Amplifier B was required to raise the mean-square signal to a level that could be read using a dc voltmeter. The mean-square measurements were recorded by a digital voltmeter with an accuracy of two decimal places. The mean-square error data used in this report were obtained by averaging some 20 mean-square readings. This variation in mean-square measurement was in the third decimal place which was negligible especially when converted into a waveform distortion reading. For example, a typical variation of 5 mV represents a change of less than 0.01 percent in the waveform distortion, $\bar{D}$.

APPENDIX E

DETAILED PROCEDURE FOR MEASURING DISTORTION

The system employed for determining waveform distortion in a telemetry channel is shown in Fig. E.1. Several preliminary adjustments are required before the waveform distortion can be determined. First, the difference amplifier must be zeroed by connecting Point C to D and adjusting the differential balance (see Appendix D) to minimize the reading on the dc voltmeter. Point C is then connected to Point A thus bypassing the telemetry system. Ideally, all the components in Data Filter A should be varied until the reading on the dc voltmeter is minimized. However, if one percent components are used and R_1 and C_o are made variable, the error is typically less than 1 mV and can be neglected. Finally, the segments of the telemetry system are adjusted according to the instructions in their respective manuals.

Upon completion of these preliminary adjustments, the waveform distortion can be measured using the following procedure.

Step 1.

Choose a pair of data filters which have a cutoff frequency at a designated percentage of the nominal bandwidth for the channel under test.

Step 2.

Turn off all the channels in the telemetry system except the test channel.

Step 3.

Adjust Attenuators A and B until the signals at points A and D are a maximum of 5 V peak to peak. This can be done by observing the signal on the oscilloscope with the slowest possible sweep speed.

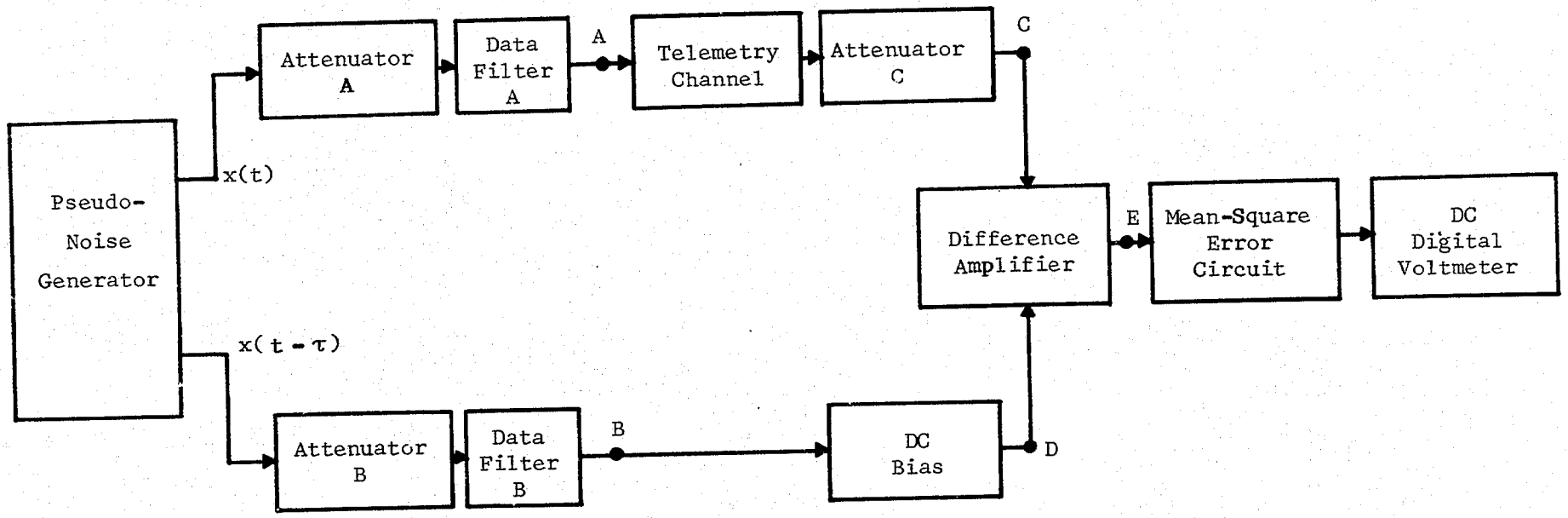

Fig. E.1. System for Measuring Waveform Distortion in an IRIG Telemetry Channel.

Step 4.

Establish a coarse or approximate time delay for the comparison signal, $x(t - \tau)$, by switching additional stages of delay in the PN sequence generator until a minimum error is read on the dc voltmeter.

Step 5.

Obtain the optimum time delay by adjusting the variable capacitor in the clock circuit. (See Appendix B.) The approach usually involves changing the capacitance until the mean-square error readings that result from the delayed signal taken from two adjacent stages of delay are approximately the same. This time delay for the minimum error is very close to the average time delay of the system.

Step 6.

Compensate for the variable power spectrum which results from varying the clcok frequency. With the time delay set to that in Step 5, adjust Attenuators A and B so that the signal at Points A and B are again 5 V peak-to-peak.

Step 7.

Establish a reference energy level by connecting Points D and E, reading the mean-square value of the data signal on the dc voltmeter, and recording this value.

Step 8.

Adjust for any error caused by gain within the system by disconnecting Point D from E, and adjusting Attenuator C until a minimum error is read on the dc voltmeter.

Step 9.

Compensate for any error caused by a difference in dc level by adjusting the dc bias until a minimum is obtained. A dual trace oscilloscope with dc response

connected to Points C and D is helpful in obtaining the correct dc bias.

Step 10.

Increase the clock frequency slightly, by decreasing the capacitance in the clock circuit of the PN generator, adjust Attenuators A and B to the same energy level as obtained in Step 7 using the same procedure as in Step 7, and repeat Steps 8 and 9. If the error decreased, then increase the clock frequency some more, and repeat Steps 8 and 9 until the error is minimized. If the error increases, then decrease the clock frequency and repeat Steps 8 and 9 until the error is minimized. The minimum error that is obtained is the mean-square value of the distortion introduced by the telemetry system for the particular bandwidth in Step 1 and a 5 V peak-to-peak data signal.

Step 11. (Optional)

Repeat Steps 6 through 10 for data signals with peak-to-peak values of 4 V, 3 V, 2 V, and 1 V.

Step 12.

Turn on the SCO for each channel and set the pre-emphasis for each channel. Load all the channels except for the test channel as follows. Load Channels 2 through 12 with a 2 Hz Square Wave and Channels 13 through 18 with a 330 Hz sinusoid.

Step 13.

Repeat Steps 6 through 11.

Step 14.

Repeat Steps 2 through 13 for other percentages of channel bandwidth.

Step 15.

Select another channel and repeat Steps 1 through 14.

APPENDIX F

WAVEFORM DISTORTION DATA FOR FM/FM TELEMETRY SYSTEM

The results for waveform distortion on Channels 2 through 18 of the IRIG FM/FM telemetry system are tabulated as a function of signal level in Tables I, II, and III. Each successive table represents data for an increasing amount of channel-bandwidth utilization by the test signal. The AN/DKT-8(XO-2) Telemetric Data Transmitting System was used as the transmitter in this experiment. The reception portion of the system consisted of a Nems Clarke Model 1674 FM receiver and a model 67F Electro-Mechanical Research Subcarrier Discriminator. The airborne system and ground station were connected by cable to eliminate any variation in waveform distortion caused by the transmission medium. The procedure for measuring the waveform distortion was described in Chapter 2. The test channel was transmitting bandlimited white noise while the others were transmitting either a square wave or sinusoid as described in Step 12 of Appendix E.

TABLE I

WAVEFORM DISTORTION FOR SMALL CHANNEL UTILIZATION

Channel	$\overline{BW}$ (%)	WAVEFORM DISTORTION (PERCENT OF FULL SCALE)					τ (ms)
		$V_m = 1$	$V_m = 2$	$V_m = 3$	$V_m = 4$	$V_m = 5$	
2	48.7	0.446	0.548	0.640	0.760	0.906	60.7
3	56.0	0.454	0.554	0.612	0.716	0.864	44.2
4	53.3	0.446	0.532	0.764	0.896	1.020	34.0
5	50.5	0.384	0.472	0.554	0.696	0.820	23.1
6	52.7	0.422	0.494	0.634	0.774	0.884	17.3
7	57.0	0.448	0.600	0.796	0.910	1.028	14.0
8	44.3	0.418	0.504	0.656	0.810	0.952	**9.58**
9	46.4	0.560	0.596	0.680	0.852	0.992	7.91
10	33.8	0.510	0.616	0.744	0.870	1.030	6.25
11	37.5	0.470	0.580	0.680	0.794	0.992	4.56
12	46.8	0.484	0.554	0.654	0.802	0.980	3.06
13	45.8	0.502	0.556	0.642	0.794	0.952	2.19
14	41.5	0.574	0.610	0.666	0.808	0.920	1.53
15	44.3	0.440	0.518	0.604	0.716	0.889	1.15
16	45.9	0.430	0.490	0.542	0.602	0.712	0.83
17	52.2	0.488	0.580	0.716	0.868	1.030	0.64
18	51.6	0.458	0.518	0.586	0.686	0.806	0.50

TABLE II

WAVEFORM DISTORTION FOR INTERMEDIATE CHANNEL UTILIZATION

Channel	$\overline{BW}$ (%)	WAVEFORM DISTORTION (PERCENT OF FULL SCALE)					τ (ms)
		$V_m = 1$	$V_m = 2$	$V_m = 3$	$V_m = 4$	$V_m = 5$	
2	66.7	0.468	0.716	0.904	1.11	1.45	61.2
3	68.2	0.488	0.712	0.860	1.13	1.39	44.6
4	72.3	0.456	0.578	0.786	0.976	1.22	34.3
5	68.5	0.430	0.578	0.764	0.948	1.17	23.7
6	76.9	0.474	0.648	0.852	1.120	1.45	17.8
7	78.4	0.496	0.716	0.916	1.230	1.52	14.3
8	61.0	0.458	0.666	0.900	1.124	1.42	9.90
9	70.0	0.650	0.742	0.906	1.192	1.39	8.00
10	69.4	0.600	0.752	0.940	1.154	1.43	6.55
11	68.2	0.512	0.670	0.904	1.00	1.17	4.69
12	69.5	0.520	0.654	0.852	1.08	1.33	3.10
13	62.3	0.472	0.628	0.824	1.04	1.31	2.26
14	60.6	0.608	0.704	0.876	1.09	1.266	1.56
15	72.1	0.502	0.658	0.874	1.11	1.39	1.18
16	68.8	0.508	0.624	0.833	1.02	1.25	0.84
17	72.4	0.526	0.692	0.856	1.06	1.31	0.64
18	68.4	0.642	0.788	0.974	1.17	1.41	0.53

TABLE III

WAVEFORM DISTORTION FOR LARGE CHANNEL UTILIZATION

Channel	$\overline{BW}$ (%)	WAVEFORM DISTORTION (PERCENT OF FULL SCALE)					τ (ms)
		$V_m = 1$	$V_m = 2$	$V_m = 3$	$V_m = 4$	$V_m = 5$	
2	87.0	0.580	0.956	1.30	1.72	2.15	61.8
3	92.7	0.576	0.862	1.26	1.66	2.08	45.2
4	97.9	0.558	0.872	1.26	1.61	2.10	34.8
5	99.5	0.536	0.966	1.39	1.77	2.25	24.3
6	96.5	0.578	0.976	1.36	1.76	2.26	18.5
7	92.8	0.642	1.070	1.52	2.07	2.54	14.4
8	91.8	0.526	0.866	1.23	1.65	2.02	10.1
9	96.6	0.690	0.986	1.35	1.69	2.08	8.25
10	92.3	0.606	0.968	1.35	1.72	2.15	6.62
11	91.8	0.788	1.020	1.30	1.60	1.92	4.73
12	100.0	0.672	1.050	1.49	1.94	2.42	3.19
13	90.5	0.576	0.852	1.22	1.61	2.01	2.30
14	82.8	0.650	0.952	1.30	1.57	1.90	1.58
15	91.8	0.624	0.920	1.25	1.62	2.03	1.19
16	93.8	0.612	0.958	1.33	1.72	2.11	0.86
17	94.7	0.620	0.952	1.34	1.75	2.18	0.65
18	92.5	0.778	1.080	1.45	1.84	2.27	0.55

REFERENCES

1. J.H. Crow, Aerospace Telemetry, Volume II, H.L. Stiltz (Ed.). New Jersey: Prentice-Hall, 1966, pp. 71-104.

2. B.M. Adair, Dynamic Error in the Frequency Modulated Telemetry System of the SATURN Space Vehicle. Master's thesis, University of Alabama, 1966, p. 99.

3. M.H. Nichols and L.L. Rauch, Radio Telemetry. New York: John Wiley and Sons, 1960, pp. 77-82.

4. J.C. Hancock, The Principles of Communication Theory. New York: McGraw-Hill, 1961, pp. 57-58.

5. Y.W. Lee, Statistical Theory of Communications. New York: John Wiley and Sons, 1960, pp. 355-360.

6. S.W. Golomb, et al., Digital Communications With Space Applications. New Jersey: Prentice-Hall, 1964, pp. 7-11.

7. T.H. Shepertycki, "Telemetry Error Measurements Using Pseudo-Random Signals," IEEE Transactions on Space Electronics and Telemetry, p. 113, September, 1964.

8. Shepertycki, op. cit., pp. 113-115.

9. R.S. Simpson and R.C. Houts, "A Definition of Average Time Delay for a Linear System," Proceedings of the IEEE, vol. 55, p. 1733, October, 1967.

10. Y.W. Lee, op. cit., pp. 331-343.

11. R.C. Houts and R.S. Simpson, "Techniques For Determining Waveform Distortion in Linear Networks," Proceedings of the IEEE Region III Convention, pp. 143-148, April, 1967.

12. N.G. Davies, "Some Properties of Linear Recursive Sequencies," Defense Research Telecommunications Establishment, DTRE Report No. 1031, pp. 1-13, December, 1959.

13. R.P. Gilson, "Some Results of Amplitude Distribution Experiments on Shift Register Generated Pseudo-Random Noise," IEEE Transactions on Electronic Computers, p. 926, December, 1966.

14. Burr-Brown Research Corporation, Handbook of Operational Amplifier Active RC Networks. Tuscon, Arizona: Burr-Brown Corporation, 1966, pp. 27-35.

15. Burr-Brown Research Corporation, Handbook of Operational Amplifier Applications. Tuscon, Arizona: Burr-Brown Corporation, 1963, p. 58.

16. Burr-Brown Research Corporation, Instruction Manual for Model 9875, High Speed Squaring Module. Tuscon, Arizona: Burr-Brown Corporation, 1967, p. 9.

COMMUNICATION SYSTEMS GROUP

RECENT REPORTS

An Exponential Digital Filter for Real Time Use, R.S. Simpson, C.A. Blackwell and W.H. Tranter, July, 1965.

An Evaluation of Possible Modifications of the Existing IRIG FM/FM Telemetry Standards, R.S. Simpson, C.A. Blackwell and J.B. Cain, May, 1966.

Analysis of Premodulation Gain in a SS/FM Telemetry System, R.S. Simpson and C.A. Blackwell, June, 1966.

Tape Recorder Flutter Analysis and Bit-Rate Smoothing of Digital Data, R.S. Simpson and R.C. Davis, June, 1966.

A Study of Redundancy in Saturn Flight Data, R.S. Simpson and J.R. Haskew, August, 1966.

AM-Baseband Telemetry Systems, Vol. 1: Factors Affecting a Common Pilot System, R.S. Simpson and W.H. Tranter, February, 1968.

Waveform Distortion in an FM/FM Telemetry System, R.S. Simpson, R.C. Houts and F.D. Parsons, June, 1968.